

A Comparative Study between Matrix Converter Fed Induction Motor Drive and Dual-Matrix Converter Fed Open-End Winding Induction Motor Drive

A. BELADEL¹, A. KOUZOU¹, A. HAFAIFA¹, S. SUNTER^{2*}, D. MAHIA³

¹ Applied Automation and Industrial Diagnostics Laboratory (LAADI), Faculty of Sciences and Technology, Djelfa University, Algeria

²Firat University, Elazig, Turkey

³University Amar Telidji of Laghouat, Algeria

*_ssunter@firat.edu.tr

(Geliş/Received: 24.02.2017; Kabul/Accepted: 12.04.2017)

Abstract

This paper deals with a comparative study between the control of three to three phase matrix converter feeding a star-connected three phase induction machine and the control of three to three phase dual matrix converter feeding an open-end winding induction machine. The control strategy used in both cases is based on a proposed direct transfer function control approach of Venturini algorithm which allows to obtain a unity power factor at the input side to boost the output phase voltage up to 150% compared to the input phase voltage, while keeping the main advantage of the matrix converter by providing a fully bidirectional power flow operation. The main objective of using the open-end winding topology is to ensure the minimization of the common mode voltage which is clearly observed in the case of star-connected winding. Simulation results are presented under both control strategies, where both matrix converters are supplied from the same three-phase power source. Whereas; the two output voltage system of the dual matrix converter are shifted with 180 degrees. Based on the obtained results the performances of the both control approaches are technically discussed.

Keywords : Matrix converter, Dual matrix converter, Direct transfer function approach, Simulation Model, Open-End Induction Machine Drive.

Açık-Uçlu Sargılı Asenkron Motoru Besleyen Çift-Matris Dönüştürücü Sürücüsü ile Asenkron Motoru Besleyen Matris Dönüştürücü Sürücüsünün Bir Karşılaştırması

Özet

Bu makale yıldız bağlı üç-fazlı asenkron motoru besleyen üç-faza üç-faz matris dönüştürücünün kontrolü ve açık-uçlu sargılı asenkron makineyi besleyen üç-faza üç-faz çift matris dönüştürücünün kontrolü ile ilgilidir. Her iki durumda kullanılan kontrol stratejisi, tam olarak çift yönlü güç akışını sağlayan matris dönüştürücünün avantajlarını koruyarak giriş faz gerilimine göre çıkış faz gerilimini %150'ye kadar yükselten ve giriş tarafında birim güç faktörü elde etmeyi sağlayan Venturini algoritmasının direkt transfer fonksiyonu kontrol yaklaşımına dayanır. Açık-uçlu sargı topolojisinin kullanılmasının ana nedeni yıldız-bağlı sargı durumunda açıkça gözlemlenen ortak mod geriliminin en aza indirilmesidir. Benzetim sonuçları her iki matris dönüştürücünün aynı üç-fazlı güç kaynağından beslendiği durumda her iki kontrol stratejisi için sunulmuştur. Çift matris dönüştürücünün iki çıkış gerilim seti 180 derece kaydırılmıştır. Elde edilen sonuçlara dayanarak her iki kontrol yaklaşımının performansları teknik olarak tartışılmıştır.

Anahtar Kelimeler : Matris dönüştürücü, Çift matris dönüştürücü, Direkt transfer fonksiyonu yaklaşımı, Benzetim modeli, Açık-uçlu asenkron makine Sürücüsü

1. Introduction

Recently, dual-matrix converter feeding open-end winding induction motor drives have

attracted great interest due to their inherent advantages compared to the standard star or delta connected induction machine drives. The main characteristics of open-end winding induction

machine are [1,2]: Since the machine is powered from both ends of the winding, each matrix converter has half of the machine power rating and therefore each stator phase current can be controlled individually. Consequently, depending on the modulation strategy, possibility of doubling the effective switching frequency is caught. The matrix converter (MC) is a forced commutated converter which can achieve varying amplitude and frequency at the output side. Indeed in recent years, significant research efforts have focused on direct matrix converter where it is increasingly used in several applications due to some implicit advantages comparing to their analogue indirect power electronics conversion using two stages power conversion, DC-AC and AC-AC. Main outstanding advantages of the matrix converter can be summarized as follows [2,3]:

1. Direct conversion (no dc link);
2. Sinusoidal input and output currents can be achieved;
3. The easiness of the input power factor control for any kind of load;
4. Bi-directional power flow capability;
5. Simple and compact design;

On the other side, due to the high integration capability of the semiconductor structures, the matrix converter topology is being recommended for several extreme and critical applications. However, the topology of the matrix converter itself has pushed the researchers to run after more favorable control strategies. In this context several modulation techniques have been developed to fulfil the requirement of the matrix converter control. Among these techniques two main control approaches are being used, the scalar approach such as; the direct transfer function approach (DTF) proposed by Venturini [4,5], and the space vector approach such as; direct and indirect space vector modulation (DSVM and ISVM) [6,7].

In this paper, the direct transfer function control approach is applied to the matrix converter for feeding an open-end three-phase load topology to overcome the main problem of the common mode voltage and to achieve a more flexible control and the operation reliability [8,9]. The both sides of the three-phase load are

supplied using dual three-phase to three-phase matrix converters. The dual matrix converter has the same topology as shown in Fig. 1. The load is an open-end winding induction machine supplied by a dual matrix converter.

In this paper, a comparison between the applications of the same induction machine supplied by a single matrix converter and a dual-matrix converter is presented. Simulation tests were performed to demonstrate the effectiveness of the used topology and control approach for both single and dual matrix converter applications for the same induction machine.

C_f limits the voltage distortion between the terminals of the converter.

L_f limits the current distortion of the supply.

R_f limits the overshoot on turn-on and avoids the resonance excitation by the supply or converter.

2. The Matrix Converter Topology

The topology of a three-phase input - three-phase output matrix converter is presented in Fig.1. The voltages V_{i1} , V_{i2} and V_{i3} are the input-voltages and V_{o1} , V_{o2} and V_{o3} are the output voltages. Each leg has three bidirectional power switches to ensure the connection between one phase of the input and one phase of the output at any instant [8].

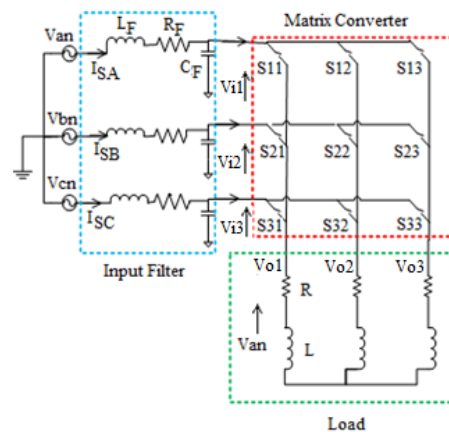


Figure 1. Three-phase matrix converter with input filter

These switches are operating under the two main constraints which are: The input side is not short-circuited and the output side cannot present an open-circuit at any instant. These are the two main important constraints that they are imposed by the normal operation of matrix converter to protect both of the matrix converter and the load [9-11].

The vector of the input voltages is given as follows:

$$\begin{bmatrix} V_{i1} \\ V_{i2} \\ V_{i3} \end{bmatrix} = V_{im} \begin{bmatrix} \cos(\omega_i t) \\ \cos(\omega_i t + 2\pi/3) \\ \cos(\omega_i t + 4\pi/3) \end{bmatrix} \quad (1)$$

The vector of the output voltages is given as follows:

$$\begin{bmatrix} V_{o1} \\ V_{o2} \\ V_{o3} \end{bmatrix} = V_{om} \begin{bmatrix} \cos(\omega_o t) \\ \cos(\omega_o t + 2\pi/3) \\ \cos(\omega_o t + 4\pi/3) \end{bmatrix} \quad (2)$$

2.1. The Switching Equations

The symbol S_{ij} represents the ideal bidirectional switches, where i ($=1, 2, 3$) represents the index of the output side and j ($=1, 2, 3$) represents the index of the input side. The relation between the output voltages and the input voltages can be achieved via an intermediate matrix M , which is known as the modulation matrix, hence the relation between the input and output voltages can be expressed as follows:

$$[V_o] = [M] \cdot [V_i] \quad (3)$$

The relation between the input current $[I_i]$ and output current $[I_o]$ can be deduced:

$$[I_i] = [M]^T \cdot [I_o] \quad (4)$$

where $[M]^T$ represents the transposed matrix of $[M]$.

Equation (3) can be presented in a developed manner as follows:

$$\begin{bmatrix} V_{o1} \\ V_{o2} \\ V_{o3} \end{bmatrix} = \begin{bmatrix} m_{11} & m_{12} & m_{13} \\ m_{21} & m_{22} & m_{23} \\ m_{31} & m_{32} & m_{33} \end{bmatrix} \begin{bmatrix} V_{i1} \\ V_{i2} \\ V_{i3} \end{bmatrix} \quad (5)$$

where the elements of the modulation matrix representing the modulation coefficients are expressed as follows:

$$m_{ij} = \frac{t_{ij}^k}{T_s} \quad (6)$$

During the switching process, the bidirectional switches can connect or disconnect the phase i of the input to the phase j of the output which is connected to the load. In general, the modulation coefficient must provide the following rules [12]:

- At any instant, only one switch S_{ij} ($i = 1, 2, 3$) conducts in order to avoid short-circuit between the input phases.

$$\sum_{i=1,2,3} S_{ij}(t) = 1; j = \{1,2,3\} \quad \forall t \quad (7)$$

- At any instant, at least two switches S_{ij} ($j = 1, 2, 3$) conduct to ensure a way to the inductive load current.
- The switching frequency $f_s = \omega_s/2\pi$ must have a higher value than the maximum of f_i, f_o ($f_s \gg \max f_i f_o$).
- During the period, T_s which is known as the sequential period, the sum of the conduction times of switches being used to synthesize the same output phase must be equal to T_s .

The time t_{ij} ; which is called the time of modulation, can be defined as:

$$t_{ij} = m_{ij} \cdot T_s \quad (8)$$

3. Modified Direct Transfer Function Approach

The modified direct transfer function approach [4,5] permits to control the switch, S_{ij} , whereas the output voltage, V_{oij} and the input current, i_{ij} are sinusoidal with the same values of the output frequency, the input amplitude, the input frequency and the displacement factor.

The maximum voltage output is obtained by the injection of the third harmonic of the output and input waveforms. The mean values of the output voltage over the sequence K^{th} are then given by:

$$\begin{aligned} v_{o1}^{(k)} &= v_{i1}^{(k)} \frac{t_{11}}{T_s} + v_{i2}^{(k)} \frac{t_{12}}{T_s} + v_{i3}^{(k)} \frac{t_{13}}{T_s} \\ v_{o2}^{(k)} &= v_{i1}^{(k)} \frac{t_{21}}{T_s} + v_{i2}^{(k)} \frac{t_{22}}{T_s} + v_{i3}^{(k)} \frac{t_{23}}{T_s} \\ v_{o3}^{(k)} &= v_{i1}^{(k)} \frac{t_{31}}{T_s} + v_{i2}^{(k)} \frac{t_{32}}{T_s} + v_{i3}^{(k)} \frac{t_{33}}{T_s} \end{aligned} \quad (9)$$

The conduction time is modulated with the ω_m while T_s is constant, such as $\omega_m = \omega_o - \omega_i$, these times are defined as follows:

1. In the first phase, we have:

$$\begin{aligned} t_{11} &= \frac{T_s}{3} (1 + 2q \cos(\omega_m t + \theta)) \\ t_{12} &= \frac{T_s}{3} \left(1 + 2q \cos(\omega_m t + \theta - \frac{2\pi}{3})\right) \\ t_{13} &= \frac{T_s}{3} \left(1 + 2q \cos(\omega_m t + \theta - \frac{4\pi}{3})\right) \end{aligned} \quad (10)$$

2. In the second phase, we have:

$$\begin{aligned} t_{21} &= \frac{T_s}{3} \left(1 + 2q \cos(\omega_m t + \theta - \frac{4\pi}{3})\right) \\ t_{22} &= \frac{T_s}{3} (1 + 2q \cos(\omega_m t + \theta)) \\ t_{23} &= \frac{T_s}{3} \left(1 + 2q \cos(\omega_m t + \theta - \frac{2\pi}{3})\right) \end{aligned} \quad (11)$$

3. In the third phase, we have:

$$\begin{aligned} t_{31} &= \frac{T_s}{3} \left(1 + 2q \cos(\omega_m t + \theta - \frac{2\pi}{3})\right) \\ t_{32} &= \frac{T_s}{3} \left(1 + 2q \cos(\omega_m t + \theta - \frac{4\pi}{3})\right) \\ t_{33} &= \frac{T_s}{3} (1 + 2q \cos(\omega_m t + \theta)) \end{aligned} \quad (12)$$

where θ is initial phase angle.

The output voltage is:

$$[V_o^{(k)}] = [M^{(k)}] \cdot [V_i^{(k)}] \quad (13)$$

$$[M^{(k)}] = \begin{bmatrix} 1 + 2q \cos(A) & 1 + 2q \cos\left(A - \frac{2\pi}{3}\right) & 1 + 2q \cos\left(A - \frac{4\pi}{3}\right) \\ 1 + 2q \cos\left(A - \frac{4\pi}{3}\right) & 1 + 2q \cos(A) & 1 + 2q \cos\left(A - \frac{2\pi}{3}\right) \\ 1 + 2q \cos\left(A - \frac{2\pi}{3}\right) & 1 + 2q \cos\left(A - \frac{4\pi}{3}\right) & 1 + 2q \cos(A) \end{bmatrix} \quad (14)$$

where

$$\begin{cases} A = \omega_m t + \theta \\ \omega_m = \omega_o - \omega_i \end{cases} \quad (15)$$

This mathematical development shows that the matrix converter with modified direct transfer function approach generates three-phase sinusoidal voltage waveforms at the output.

4. Modelling of the Open-End Winding Induction Machine

The open-end stator winding induction machine presented in Fig. 2 is supplied by two three-phase voltage systems and these systems are defined as:

The three-phase systems supplied by the first matrix converter: $[V_{s1}] = [V_{s11} \ V_{s12} \ V_{s13}]^T$;

The three-phase systems supplied by the second matrix converter: $[V_{s2}] = [V_{s21} \ V_{s22} \ V_{s23}]^T$;

Hence, the voltage vector applied on the stator winding of the machine is:

$$[V_s] = [V_{s11} - V_{s21} \ V_{s12} - V_{s22} \ V_{s13} - V_{s23}]^T$$

The mathematical flux model is defined in (d-q) reference frame, and described by the following state equations representation:

$$\frac{dX(t)}{dt} = [A(\omega, \omega_{dq})][X(t)] + [B] \cdot U(t) \quad (16)$$

$$Y(t) = [C] \cdot Y(t) \quad (17)$$

where

$X(t) = [\phi_{sd} \ \phi_{sq} \ \phi_{rd} \ \phi_{rq}]$ is the state vector;

$U(t) = U_1(t) - U_2(t) = [V_{sd1} - V_{sd2} \ V_{sq1} - V_{sq2}]$ is the control vector;

$Y(t) = [I_{sd} \ I_{sq} \ I_{rd} \ I_{rq}]$ is the output vector.

The principle diagram of the system is shown in Fig. 2:

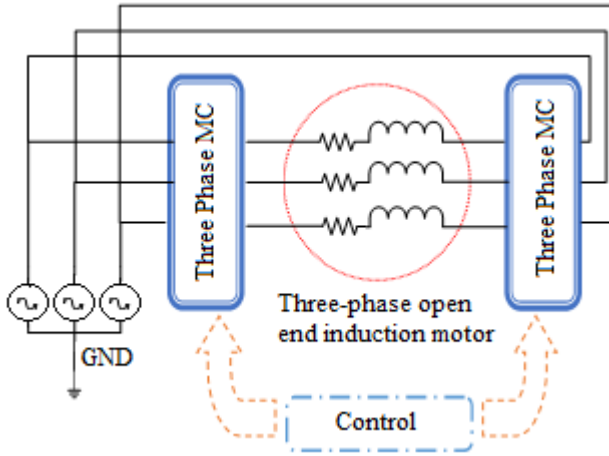


Figure 2. Three phase open-end winding induction motor fed by dual matrix converter

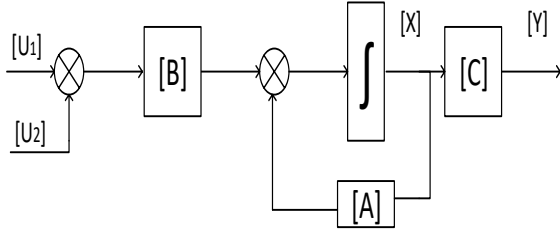


Figure 3. Block diagram of the open-end winding machine

On the other side the following parameters are taken into account:

$\tau_s = \frac{L_s}{R_s}$ is the stator constant time

$\tau_r = \frac{L_r}{R_r}$ is the rotor constant time

$\sigma = 1 - \frac{M_{sr}^2}{L_s L_r}$ is the coefficient of dispersion of Blondel

R_r is the rotor resistance, R_s is the stator resistance, L_r is the rotor inductance, L_s is the stator inductance, M_{sr} is the mutual inductance between stator and rotor.

The equation for current vector is

$$[I] = [L]^{-1}[\Phi] \quad (18)$$

The matrices [A], [B] and [C] are defined as follows:

$$[A] = \begin{bmatrix} -\frac{1}{\sigma\tau_s} & \omega_{dq} & \frac{M_{sr}}{\sigma\tau_s L_r} & 0 \\ -\omega_{dq} & -\frac{1}{\sigma\tau_s} & 0 & \frac{M_{sr}}{\sigma\tau_s L_r} \\ \frac{M_{sr}}{\sigma\tau_r L_s} & 0 & -\frac{1}{\sigma\tau_r} & \omega_{dq} - \omega \\ 0 & \frac{M_{sr}}{\sigma\tau_r L_s} & -(\omega_{dq} - \omega) & -\frac{1}{\sigma\tau_r} \end{bmatrix} \quad (19)$$

$$B = \begin{bmatrix} 1 & 0 & 0 & 0 \\ 0 & 1 & 0 & 0 \\ 0 & 0 & 1 & 0 \\ 0 & 0 & 0 & 1 \end{bmatrix}$$

$$[C] = [L]^{-1} = \begin{bmatrix} \frac{1}{\sigma L_s} & 0 & \frac{M_{sr}}{\sigma L_s L_r} & 0 \\ 0 & -\frac{1}{\sigma\tau_s} & 0 & \frac{M_{sr}}{\sigma L_s L_r} \\ -\frac{M_{sr}}{\sigma L_r L_s} & 0 & -\frac{1}{\sigma L_r} & 0 \\ 0 & -\frac{M_{sr}}{\sigma L_r L_s} & 0 & \frac{1}{\sigma L_r} \end{bmatrix} \quad (20)$$

The mechanical equation is given as follows:

$$T_{em} - T_r = j \frac{d\omega}{dt} + f\omega \quad (21)$$

$$T_{em} = \frac{3}{2} p (\Phi_{sa} I_{s\beta} - \Phi_{s\beta} I_{sa}) \quad (22)$$

where T_{em} is the electromagnetic torque; T_r is the load torque.

5. Simulation

In this work, two simulation tests were performed to prove the advantage of the use of the open-end winding induction machine fed by a dual matrix converter having the same topology and characteristic. The first simulation presents the induction machine fed by only one matrix converter, where the output voltage is characterized by a fundamental frequency of $f_0=50$ Hz and a magnitude of $V_0=350$ V. The parameters of the input voltage source and the induction machine are presented in Table 1. On the other side, due to the distortion which may occur in the input current and to avoid the propagation of this kind of harmonics pollution toward the source, an LC input filter is inserted as shown in Fig.2 where its parameters can be found in Table 1. [13-15].

5.2. Induction Motor Fed by A Three-Phase Matrix Converter

In this case, a single three-phase matrix converter is used to feed a three-phase induction motor. The output voltage and the output current of the matrix converter are presented in Fig. 4 and 6, respectively. Total Harmonic Distortion (THD) of the output voltage and current waveforms, which is defined in Eq. (23), are presented in Fig. 5 and 7, respectively. It can be concluded that the harmonic rays are around the switching frequencies ($n \times f_s$) where it is taken as $f_s=10$ kHz

$$THD = \sqrt{\frac{V_2^2 + V_3^2 + \dots + V_n^2}{V_1^2}} \quad (23)$$

The fundamental harmonic amplitude of the output voltage is 344.4 V with THD of 99.36% as shown in Fig. 5 and harmonics rays can be remarked clearly around the switching frequency. However, due to the inductive nature of the induction motor, the output current poses a low THD as 2.77%. Figs. 8 and 9 show the decoupling carried out between the flux and the electromagnetic torque. The decoupling between torque and machine speed is remarked clearly especially at the interval between 1.5 s and 2.5 s. The supply current waveform is shown in Fig.10. The result shows great effect of the input filter where the high order harmonics are eliminated by the input filter.

Table 1. Simulation parameters

V_s	Input voltage	350 V
f_s	Input frequency	50 Hz
L_f	Filter inductance	0.03 H
R_f	Filter Resistance	0.5 Ω
C_f	Filter Capacitance	25 μ F
R_s	Stator resistance	4.85 Ω
R_r	Rotor resistance	3.81 Ω
L_s	Stator inductance	0.274 H
L_r	Rotor inductance	0.274 H
L_m	Mutual inductance	0.258 H

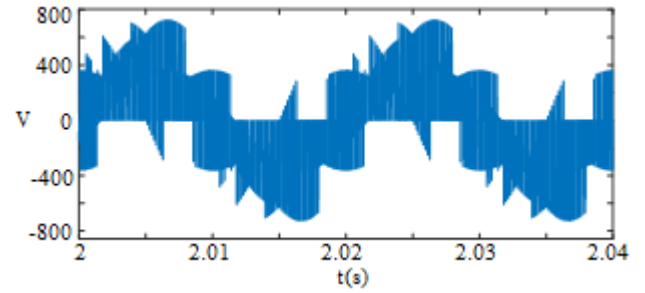


Figure 4. Output line voltage waveform of the matrix converter

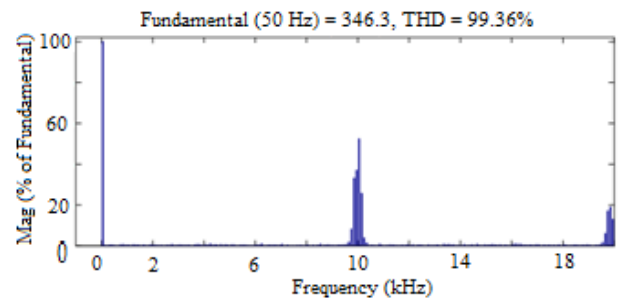


Figure 5. Harmonic spectrum of the matrix converter output voltage waveform

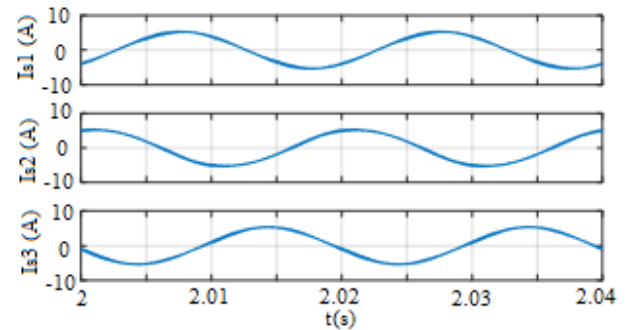


Figure 6. Three-phase motor currents

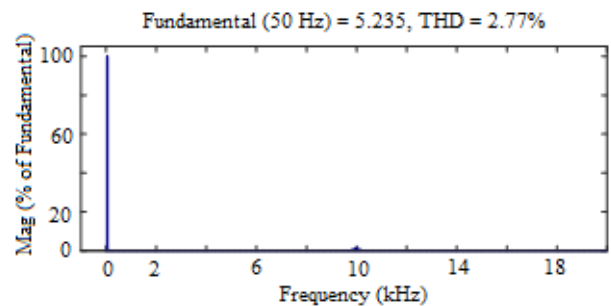


Figure 7. Harmonic spectrum of the matrix converter output current

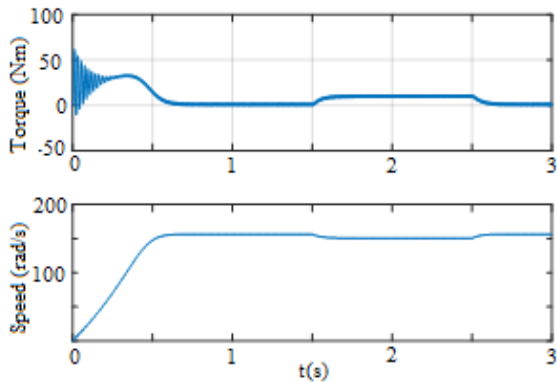


Figure 8. Torque (up) and speed (bottom) of the induction motor

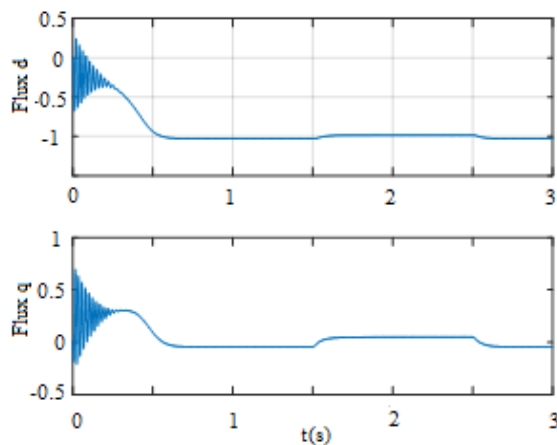


Figure 9. Flux flowing rotor axis "d" (up) and flux flowing rotor axis "q" (bottom)

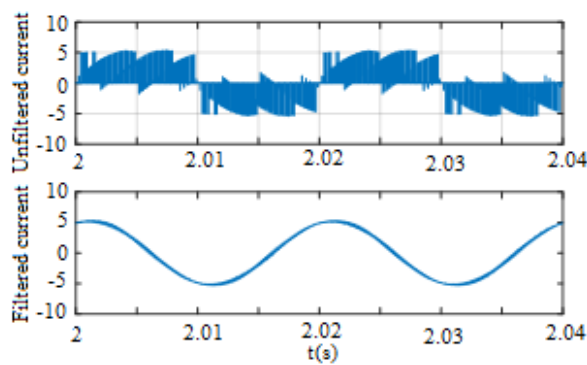


Figure 10. The supply current without and with filtering, respectively

5.2. Dual Matrix Converter Feeding Open-End Winding Induction Motor

In this case, two of three-phase matrix converter feed the both sides of the open-end winding of the same induction machine stated previously. Under this topology the common mode voltage (CMV) will be totally removed and the three-phase load can be controlled

independently. Due to the balanced nature of the load, the voltage applied at each load phase is the same except for the eventual required phase shift. Figs.11 and 12 illustrate the voltages between the two terminals of the three-phase load and the load currents, respectively. It is obvious that the fundamental magnitude of the voltage is 348.5 V with a THD of 75.12 % whereas, the fundamental current is 4.636 A with THD of 3.36 % which means that there is an improved voltage and current quality in comparison with the situation where the machine is fed by a single three-phase matrix converter (Fig. 13 and Fig. 14). In the same time a less harmonic rays can be remarked clearly near the switching frequency $f_s = 10$ kHz. The two level voltages is clearly observed and the three-level voltage at the load terminals is also obviously observed. The effect of the input filter can be seen clearly in Fig. 17., Figs.15 and 16 show the decoupling carried out between the flux and the electromagnetic torque. In the same time, the decoupling between the torque and the speed of the machine can be seen especially at the interval between 1.5 s and 2.5 s.

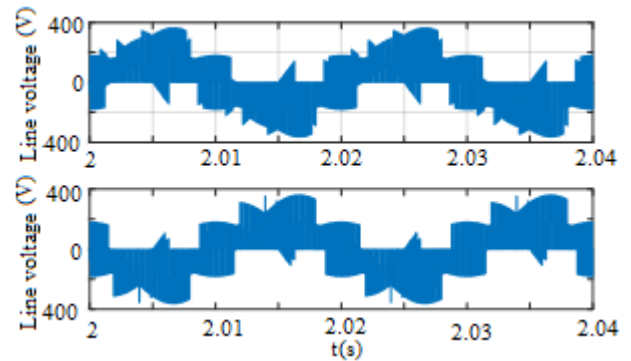


Figure 11. Output line voltage waveforms of MC1 (up) and MC2 (bottom)

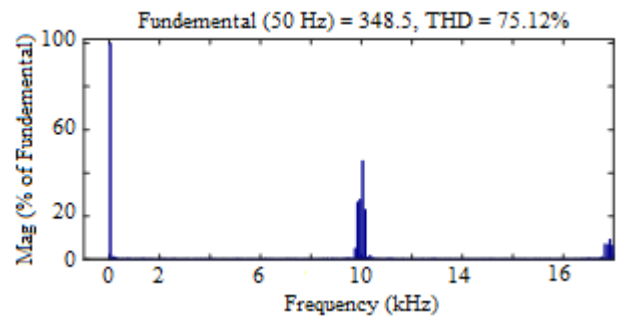


Figure 12. The Harmonic spectrum of the output voltage applied to one phase of the induction motor

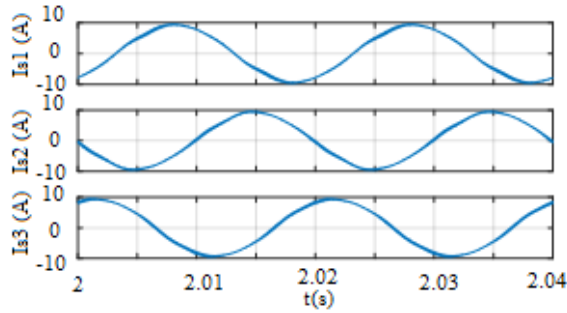


Figure 13. Three-phase motor currents

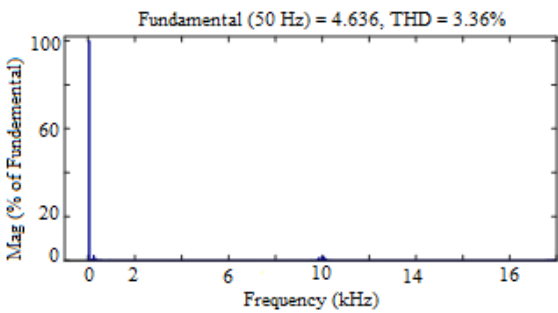


Figure 14. Harmonic spectrum of the output current

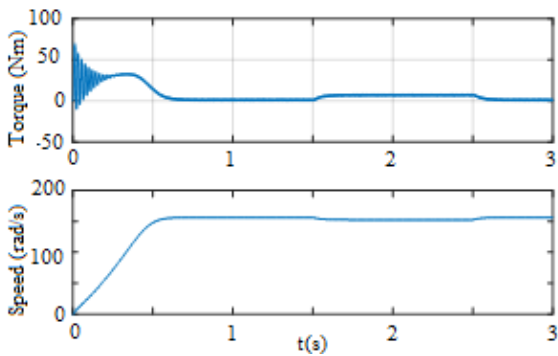


Figure 15. Torque (up) and speed (bottom) of the induction motor

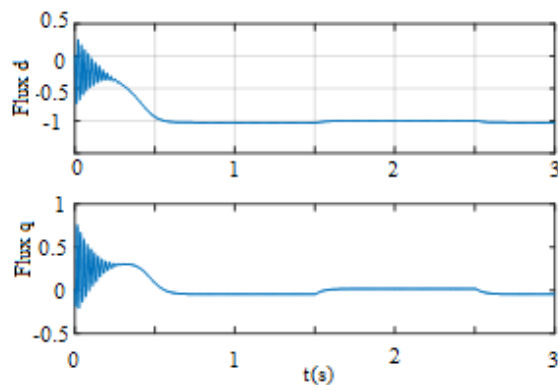


Figure 16. Flux flowing rotor axis "d" (up) and flux flowing rotor axis "q" (bottom)

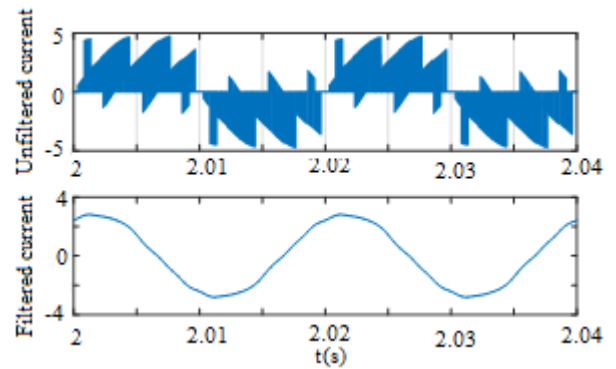


Figure 17. The supply current without and with filtering, respectively

6. Conclusions

In this paper, the main advantages of the dual matrix converter used in open-end structure are proved by simulation results. The results show clear improvement on quality of the voltages enforced to the induction machine drive and elimination of the common mode voltage which is major problem in all three-phase load applications, especially in three-phase electrical machines. On the other side, due to the multilevel nature of the voltage applied at the terminal of the open-end load, the current quality is also improved, where the THD is decreased at nearly 48% compared to the classical topology based on one matrix converter. An important issue is that the use of a dual matrix converter is more reliable in case of fault on one or more switches. This problem can be solved by easily adjusting control signals of the switches. Finally, it can be said that the presented topology can have a large use in electric machines application in industry based on the afore-mentioned advantages.

7. References

1. Riedemanna, J., Andradeb, I., Peñab, R., Blasco-Gimenezc, R., Clare J., Melin, P., Rivera, M. (2016). Modulation strategies for an open-end winding induction machine fed by a two-output indirect matrix converter, *Mathematics and Computers in Simulation*, 144-152.
2. Wheeler, P.W., Rodriguez P.W., Clare, J.C., Empringham, L., Weinstein, A., (2002). Matrix converters: A technology review. *IEEE Transactions on Industrial Electronics*, 49(2), 276-288.

3. Vargas, R., Rodríguez, J., Ammann, U., Wheeler, P.W. (2008). Predictive current control of an induction machine fed by a matrix converter with reactive power control. *IEEE Transactions on Industrial Electronics*, **55**(12), 4362-4371.
4. Venturini, M. (1980). A new sine wave in sine wave out, conversion technique which eliminates reactive elements. *POWERCON 7*, E3-1-E3-15.
5. Alesina, A., Venturini, M. (1989). Analysis and design of optimum-amplitude nine-switch direct AC-AC converters, *IEEE Transactions on Power Electronics*, **4**(1), 101-112.
6. Ahmed, S.M., Abu-Rub, H., Kouzou, A. (2013). Predictive simultaneous power and current control in a three-phase direct matrix converter. *International Conference on Power Electronics and Their Applications (ICPEA)*, Djefia-Algeria.
7. Bachir, G., Bendiabdellah, A. (2009). A comparative study between two control strategies for matrix converter. *Advances in Electrical and Computer Engineering*, **9**(2), 23-27.
8. Beladel, A., Kouzou, A., Hafifa, A., Mahia D., (2016). Dual matrix converter feeding an open-end winding load based on modified direct transfer approach, *International Scientific Conference on Engineering, Technologies and Systems*.
9. Altun, H., Sünter, S. (2003). Matrix converter induction motor drive: modeling, simulation and control. *Electrical Engineering*, **86**(1), 25-33.
10. Rodriguez, J., Silva, E., Wheeler, P., (2013). Matrix converter controlled with the direct transfer function approach: analysis, modelling and simulation, *International Journal of Electronics*, 63-85.
11. Djahbar A., Mazari B., (2007). High performance motor drive using matrix converter, *Acta Electrotechnica et Informatica*, **2**(7).
12. Guizana, S., Ammar, F.B., (2005). Dual open-end stator winding induction machine fed by redundant voltage source inverters, *Turkish Journal of Electrical Engineering & Computer Sciences*, **92**(2), 2171-2181.
13. Riedemann, J., Clare, J.C., Wheeler, P.W., Blasco-Gimenez, R., Rivera, M., Pena, R. (2016). Open-end winding induction machine fed by a dual-output indirect matrix converter. *IEEE Transactions on Industrial Electronics*, **63**(7), 4118-4128.
14. Gopal, M., Gopakumar, K., Tekwani, P.N., Emil, L.A., (2007). Reduced-switch-count five-level inverter with common-mode voltage elimination for an open-end winding induction motor drive, *IEEE Transactions on Industrial Electronics*, **54**(4).
15. Elbar, M., Mahmoudi, M.O., Naas, B., (2010). A Carrier-Based PWM Techniques Applied to a Three-Level Four-Leg Inverter For Use as a Shunt Active Power Filter, *J. Electrical Systems*, Special Issue (2), 47-57.